

Protection of animals against devastating RNA viruses using CRISPR-Cas13s

Adnan Asadbeigi,¹ Mohammad Reza Bakhtiarizadeh,² Mojtaba Saffari,³ Mohammad Hossein Modarresi,³ Naser Sadri,⁴ Zahra Ziafati Kafi,⁴ Hassan Fazilaty,⁵ Arash Ghalyanchilangeroudi,⁴ and Hossein Esmaeili⁴

¹Cancer Institute, Department of Medical Genetics, Faculty of Medicine, Tehran University of Medical Sciences (TUMS), Tehran 1417613151, Iran; ²Department of Animal and Poultry Science, College of Aburaihan, University of Tehran, Tehran 3391653755, Iran; ³Department of Medical Genetics, Faculty of Medicine, Tehran University of Medical Sciences (TUMS), Tehran 1417613151, Iran; ⁴Department of Microbiology and Immunology, Faculty of Veterinary Medicine, University of Tehran, Tehran 1419963111, Iran; ⁵Department of Molecular Life Sciences, University of Zurich, 8057 Zurich, Switzerland

The intrinsic nature of CRISPR-Cas in conferring immunity to bacteria and archaea has been repurposed to combat pathogenic agents in mammalian and plant cells. In this regard, CRISPR-Cas13 systems have proved their remarkable potential for single-strand RNA viruses targeting. Here, different types of Cas13 orthologs were applied to knockdown foot-and-mouth disease virus (FMDV), a highly contagious disease of a wide variety of species with genetically diverse strains and is widely geographically distributed. Using programmable CRISPR RNAs capable of targeting conserved regions of the viral genome, all Cas13s from CRISPR system type VI (subtype A/B/D) could comprehensively target and repress different serotypes of FMDV virus. This approach has the potential to destroy all strains of a virus as targets the ultra-conserved regions of genome. We experimentally compared the silencing efficiency of CRISPR and RNAi by designing the most effective short hairpin RNAs according to our developed scoring system and observed comparable results. This study showed successful usage of various Cas13 enzymes for suppression of FMDV, which provides a flexible strategy to battle with other animal infectious RNA viruses, an underdeveloped field in the biotechnology scope.

INTRODUCTION

Pathogenic RNA viruses are responsible for a significant proportion of animal diseases and have the potential to cross the species barrier and infect humans. For most RNA virus infections, there are no approved US Food and Drug Administration (FDA) vaccines or antiviral drugs.¹ Moreover, available antiviral medications often have limited efficacy and a narrow therapeutic window, meaning they can only reduce the severity of the infection and must be administered within a short time frame.² Therefore, new strategies are needed to treat infection of RNA viruses.

One of the most infectious RNA viral diseases of domestic and wild cloven-hoofed animals is foot-and-mouth disease (FMD) that is capable of infecting cattle, sheep, goats, pigs, buffalo, and Asian and African elephants. The causative agent, foot-and-mouth disease virus (FMDV), belongs to the genus *Aphthovirus* of the Picornaviridae

family, including seven different serotypes named O, A, C, Asia 1, Southern African Territories 1 (SAT 1), SAT 2, and SAT 3.³ Due to the high financial impact of FMD outbreaks, it can cause a significant economic loss and lead to a serious global challenge.⁴ FMD has a morbidity rate of nearly 100%, typically a 1%–5% mortality rate in adults and can lead to death in young animals due to myocarditis (inflammation of the heart muscle).⁵

Regular vaccination is the most effective strategy to prevent FMD, as there is no specific treatment available for this disease. Besides vaccination, disease control also requires effective surveillance through early detection, as well as movement restrictions and farm quarantines to prevent the further spread of the disease.⁶ Although conventional inactivated FMD vaccines can protect animals from infection, they have a number of disadvantages. (1) Vaccinated animals may still have viral replication in their oropharynx without showing any symptoms, which can make them carriers of the virus and trigger outbreaks.^{7–9} (2) Large quantities of virulent and wild-type FMD virus are needed for traditional FMD vaccines; in such a situation, incomplete inactivation of virus during vaccine formulation process or the escape of infectious virus from manufacturing facilities is possible.¹⁰ (3) High-potency vaccines require 7–10 days to generate protective immunity against direct challenge with the virus and during this time, animals will be vulnerable.¹¹ Other shortcomings include short-term protection, multiple vaccinations for obtaining good levels of immunity, need for high-biosafety production facilities, short shelf life, and problems of some serotypes and subtypes to grow in cell cultures for vaccine production.⁸

The other important problem of the current FMD vaccines originates from high mutation rates of FMDV genomes during replication that allows viruses to evolve continuously and adapt to new environments.

Received 14 December 2023; accepted 29 May 2024;
<https://doi.org/10.1016/j.omtn.2024.102235>.

Correspondence: Mohammad Reza Bakhtiarizadeh, Department of Animal and Poultry Science, College of Aburaihan, University of Tehran, Tehran 3391653755, Iran.

E-mail: mrbakhtiari@ut.ac.ir



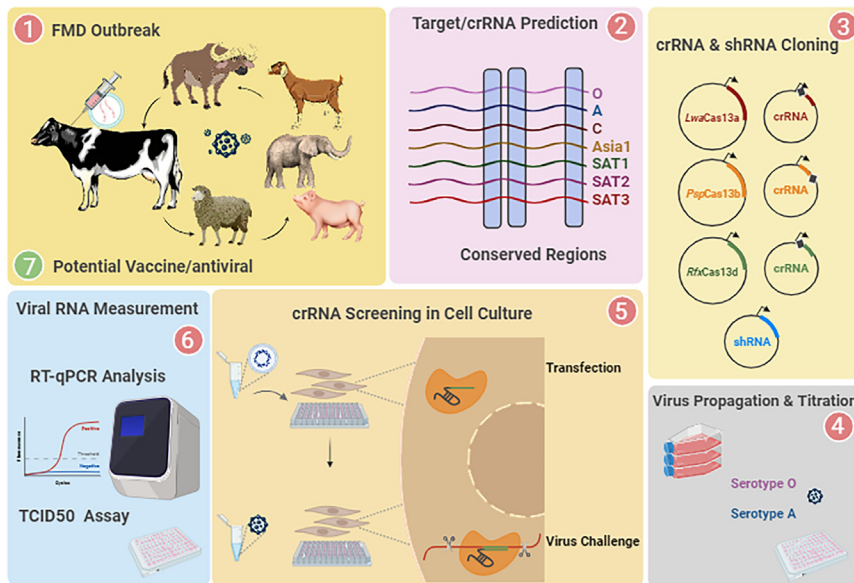


Figure 1. Schematic workflow of the used approach in this study to inhibit FMDV infection using the CRISPR-Cas system

(1) Transmission and circulation of FMD disease between wildlife-livestock ecosystems due to animal interactions. (2) Finding conserved regions among different FMDV serotypes by considering multiple criteria and designing efficient and specific crRNAs by the CaSilico tool. (3) Designed crRNAs of type VI-A/B/D were synthesized as DNA oligos, and then, each crRNA was cloned into separate crRNA cloning backbones. In addition to crRNA designing, several shRNAs were designed to compare virus knockdown by RNAi and CRISPR-Cas systems. (4) Virus propagation and titration of two FMDV serotypes (O and A) were performed on BHK-21 cells to be used for viral challenge. (5) The sgRNA screening was performed to validate potent crRNAs. (6) Two methods, RT-qPCR and TCID₅₀ assay were used to measure viral RNA and FMDV infectivity, respectively. (7) CRISPR-Cas systems can potentially be leveraged to aid antiviral development for viral diseases in animals. Figure was created with [BioRender.com](https://www.biorender.com).

FMDV serotypes exhibit considerable diversity, especially among viruses from different regions of the world. Nucleotide sequence analysis revealed that different topotypes of the virus serotypes (except for Asia 1 serotype) are distributed in distinct geographical regions. All of the seven immunologically distinct serotypes of FMDV can cause FMD infection. Immunity against each serotype, either by vaccination or recovery from infection, does not confer protection for other serotypes and sometimes against other subtypes within the same serotype.⁶ Despite the efforts to develop novel FMD vaccines, such as attenuated and marker inactivated vaccines, recombinant protein vaccines, virus-like particles (e.g., adenovirus vector, nucleic acid, and chimeric vaccines),¹² synthetic peptide vaccines, and recombinant empty capsids,¹³ many of the problems of inactivated vaccines still persist.^{9,14} Therefore, FMDV remains a major threat to the food security of the world and there is an urgent need for a fast, sensitive, and precise method to detect FMDV and protect the animals from infection.

In recent years, CRISPR-Cas (clustered regularly interspaced short palindromic repeats-CRISPR-associated protein)-based approaches have been developed to combat viral infections and to overcome the drawbacks of conventional vaccines. Compared with traditional vaccines and antiviral drugs, CRISPR-based methods have various benefits. They do not require biological perspectives of viruses and virus-host interplay, which could slow vaccine and antiviral development, especially in the face of emerging outbreaks. Among different types of CRISPR-Cas systems, Cas13 has been harnessed for RNA targeting.¹⁵ This type employs crRNAs (CRISPR RNAs) that contain a customizable spacer sequence and a Cas protein that is directed toward specific RNA molecules for targeted degradation. Several studies point to the potential of Cas13 variants to target and suppress viral sequences in various conditions^{16–18}; however, it

remains unclear whether this approach can be employed to effectively target and cleave FMDV with enormous genetic and phylogenetic diversity.

Here, crRNAs belonging to class II of the CRISPR system (type VI-A/B/D) were employed to investigate whether it is possible to extend its use to inhibit FMDV (Figure 1). We hypothesize that this system could target FMD infection by degrading the viral RNA genome. Unlike most previous studies, our approach aims to develop a strategy that can target multiple FMDV serotypes at once through specifically targeting highly conserved regions. To identify potential Cas13 target sites, we developed CaSilico¹⁹ to design crRNAs that target conserved regions of all FMDV serotypes. This approach was experimentally tested in baby hamster kidney (BHK-21) cells by live O and A serotypes and was compared with short hairpin RNAs (shRNAs). The CRISPR approach effectively reduced viral loads in BHK-21 cells, demonstrating the ability of CRISPR to achieve reprogrammable inactivation of the viral genome and block infection. The CRISPR system offers some advantages over RNAi, rendering it more suitable for therapeutic applications. For example, it generates less off-target effects, can target various subcellular compartments (such as nucleus, cytosol, and others), and has the capability to prevent the virus from evading the antiviral systems, unlike RNAi.^{15,17,20–22} Our results highlighted the potential of Cas13 to target different FMDV serotypes and as a new antiviral strategy can be extended to emerging pathogenic viruses with no effective vaccines or pharmaceuticals.

RESULTS

Designing crRNA/shRNA

Based on the 1D gene sequences of FMD representative strains, a phylogenetic tree was constructed that showed high diversity of FMD strains (supplemental information, Figure S1). Hence, to

Table 1. Spacers and shRNA sequences were used in this study for FMDV knockdown in BHK-21 cells

System	Name	Target sequence	Spacer or shRNA sequence
CRISPR-Cas (type VI-A)	L3D1	5'AGCTACAGATCACTTTACCTGCGTTGGG3' (nt 8069–8096) ^a	5'CCCAACGCAGGTAAAGTGATCTGTAGCT3'
	L3D2	5'CTTTACCTGCGTTGGGTGAACGCCGTGT3' (nt 8081–8108)	5'ACACGGCGTTACCCAACGCAGGTAAAG3'
	L3D3	5'TTTACCTGCGTTGGGTGAACGCCGTGT3' (nt 8082–8109)	5'CACACGGCGTTACCCAACGCAGGTAAA3'
	LNTC ^b	NA ^c	5'ATGTAGAAGTTTCACTTAGAAGCGCGTA3'
CRISPR-Cas (type VI-B)	P3D1	5'CAGATCACTTTACCTGCGTTGGGTGAACGC3' (nt 8074–8103)	5'GCGTTCACCCAACGCAGGTAAAGTGATCTG3'
	P3D2	5'TCACTTTACCTGCGTTGGGTGAACGCCGTGT3' (nt 8078–8107)	5' ^d G ^d CACGGCGTTACCCAACGCAGGTAAAGTGA3'
	P3D3	5'CACTTTACCTGCGTTGGGTGAACGCCGTGT3' (nt 8079–8108)	5' ^d G ^d ACACGGCGTTACCCAACGCAGGTAAAGTGT3'
	PNTC	NA	5'GCATCAATTGTCCAATACTTAGGTGCTACA3'
CRISPR-Cas (type VI-D)	R3D1	5'TCTCCTTTGCACGCCGTGGGAC3' (nt 7944–7965)	5'GTCCCACGGCGTGCAAAGGAGA3'
	R3D2	5'AGCTACAGATCACTTTACCTGCG3' (nt 8069–8090)	5'GCAGGTAAAGTGATCTGTAGCT3'
	R3D3	5'GCTACAGATCACTTTACCTGCG3' (nt 8070–8091)	5'CGCAGGTAAAGTGATCTGTAGCT3'
	RNTC	NA	5'GGGTTTCTCTACTCAATACTC3'
RNAi	sh2B	5'CITGAGATTCTGGACAGCA3' (nt 4265–4283)	5' ^d G ^d CTTGAGATTCTGGACAGCACTCGAG ^e TGCTGTCCAGAATCTCAAG3'
	sh2C	5'CTGACCACTTCGACGGTTA3' (nt 4878–4896)	5' ^d G ^d CTGACCACTTCGACGGTTACTCGAGTAACCGTCGAAGTGGTCAG3'
	sh3D	5'GCTACAGATCACTTTACCT3' (nt 8070–8088)	5'GCTACAGATCACTTTACCTCTCGAGAGGTTAAAGTGATCTGTAGCT3'
	SNTC	NA	5'GTAGCATCCCATGGTAAAGTCTCGAGACTTACCATGGATGCTAC3'

Site of sequence was obtained from the NCBI reference genome.

^aTarget sequence position on the FMDV genome. Numbering is based on alignment result of FMD representative strains with complete genomic sequences.

^bNo template control.

^cNot applicable.

^dAn additional "G" is added to the sequence to enable efficient transcription initiation by the RNA Polymerase III.

^eshRNA loop is shown as underlined text.

identify the most conserved genes in the FMDV genome, gene identity and homology percentage for each gene in the genome was calculated. The genome of FMDV is a single-stranded, positive-sense RNA with a size of around 8.4 kb. It encodes four structural proteins (VP4, VP2, VP3, and VP1) and eight non-structural proteins (L^{P^{ro}}, 2A, 2B, 2C, 3A, 3B, 3C^{P^{ro}}, and 3D^{P^{ol}}).³ The conservation analysis identified 2A, 2B, 2C, and 3D genes as the most conserved genes, which could be used to be targeted by crRNA/shRNA (supplemental information, Table S1). These genes play important roles in different phases of the viral replication cycle. The 2A gene is involved in viral assembly and maturation. FMDV 3D is a viral RNA-dependent RNA polymerase that catalyzes the replication of RNA from the RNA genome. The 2B gene activates autophagy by inducing damage to the integrity of the host cell's membrane and the 2C gene is responsible for viral replication complex and membrane rearrangement.^{23,24} Of these, 2B, 2C, and 3D genes were chosen for shRNA designing and 3D was considered as the target gene for designing crRNA molecules, as it has long conserved regions.

CaSilico¹⁹ was used to find the conserved regions in the 3D gene sequences of different FMD strains. We set the conservation threshold to 96% and used a sliding window method with a stride of one nucleotide to identify all the potential target sites for CRISPR-Cas13a/b/

day. In sum, 76, 29, and 121 candidates were designed for *Lwa*Cas13a, *Psp*Cas13b, and *Rfx*Cas13d, respectively (Table S3). A set of three 28-nt *Lwa*Cas13a crRNAs (L3D1, L3D2, L3D3), three 30-nt *Psp*Cas13b crRNAs (P3D1, P3D2, P3D3), and three 22-nt *Rfx*Cas13d crRNAs (R3D1, R3D2, and R3D3) were selected from the suggested candidates to target the 3D gene (Table 1; Figure 2). This set was selected based on their features including number of mismatches, frequency of cleaving base around the target site, target accessibility, self-complementarity, and off-target analysis. This set of crRNAs provided a broad-genotypic coverage of FMDV that guards targeting activity against mutational escape.

There are a large number of tools available that consider multiple criteria for designing shRNA, but there is no tool that can ensure the effectiveness of an shRNA. Also, unlike CaSilico that detects conserved regions among the provided sequences, these tools only design shRNA to target one sequence. To overcome these problems and increase knockdown efficiency, shRNAs were designed based on the results of seven tools (especially those developed based on linear regression models and artificial neural networks) and processed as described in materials and methods. In total, 19, 12, and 50 candidates were designed to target 2B, 2C, and 3D genes, respectively (Table S4). All shRNAs are assigned a predicted efficiency

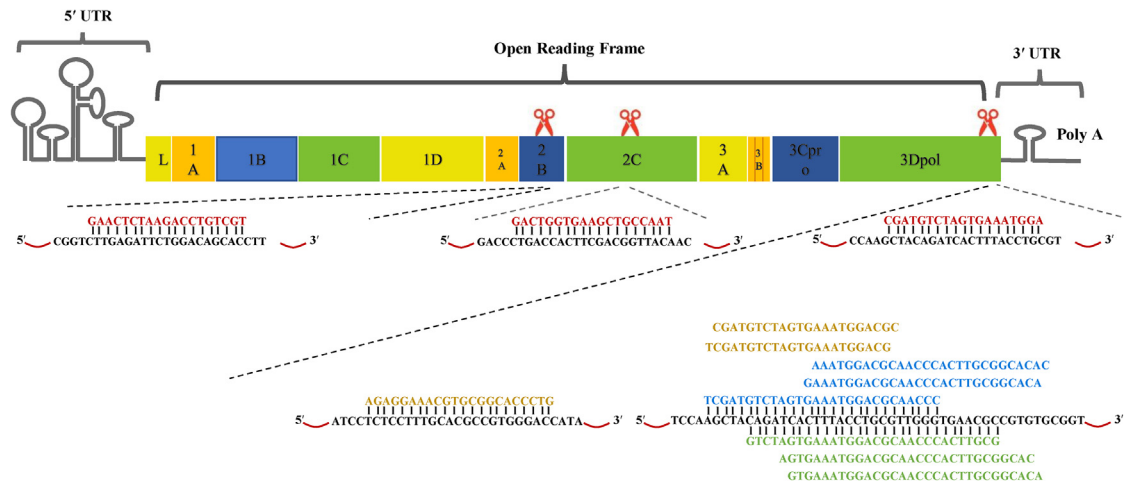


Figure 2. Schematic of FMDV genome and targeted regions by CRISPR-Cas and RNAi systems

Scissors indicate target sites. Conserved regions of the 3D gene were tiled with nine crRNAs belonging to different subtypes of CRISPR-Cas type VI. *Lwa*Cas13a, *Psp*Cas13b, and *Rfx*Cas13d spacers are indicated in blue, green, and orange, respectively. The nucleotides in red highlight residues in the guide (antisense) strand of shRNA. Proper non-targeting controls as negative control “scramble” for nonspecific effects were designed. NTCs have the shuffled nucleotide sequence of the target-specific crRNA or shRNA and have passed characteristics of a functional crRNA or shRNA such as off-target analysis (Table 1).

score based on the scoring system. shRNAs with higher scores, preferentially without mismatches and designed by different tools, were chosen for experimental analysis. After applying our scoring system, one shRNA was selected for targeting each gene (Table 1, Figure 2).

Cas13 is capable of suppressing FMDV replication in infected cells

After computational screening for crRNAs, the potential of Cas13 as a wide-range antiviral strategy was evaluated in viral infection using the BHK-21 cell line. This cell line is most commonly used in production of the FMDV vaccine. For this purpose, Cas13a/b/day effectors and crRNAs were expressed using separate plasmids (materials and methods). Three targeting crRNAs and one non-targeting crRNA control were used for each Cas13 to assess viral genome cleavage activity (Table 1). To test multiplexing efficiency that can target different regions of viral RNA to increase robustness of knockdown and mitigate the risk of *in vivo* target inaccessibility, three individual crRNAs for each subtype were pooled and transfected into the BHK-21 cells. In each subtype of the type VI CRISPR system, individual or pooled crRNAs and relative Cas13 enzyme encoding plasmids co-transfected into BHK-21 cells to measure the inhibitory effects of crRNAs on FMD RNA replication (Figure 3A). Since serotype O is responsible for most of the FMDV outbreaks worldwide, viral challenge was carried out 24 h post transfection (hpt) by this serotype.²⁵ Supernatant from infected cells was collected 24 h post infection (hpi) and viral RNA abundance was quantified by RT-qPCR. As shown in Figure 3B, all L3D crRNAs efficiently lowered viral copy numbers compared with control crRNA. Of these, L3D3 was the most effective crRNA that inhibited FMDV infection by the CRISPR-Cas13a system ($p < 0.01$, $p < 0.01$, and $p < 0.001$, for L3D1, L3D2, and L3D3, respectively).

Results of the Cas13b-mediated inhibition of FMDV replication revealed that viral RNA levels were significantly lower in the supernatant of treated cells with P3D1 and P3D3 crRNAs relative to control crRNA ($p < 0.0001$ and $p < 0.0001$, respectively, Figure 3C). In *Rfx*Cas13d, only R3D2 crRNA significantly decreased the levels of FMDV viral RNA in comparison with control crRNA ($p < 0.01$, Figure 3D). Among the different Cas13 crRNAs, P3D3 crRNA showed the highest efficiency to inhibit FMDV infection, as approximately none of FMDV viral RNAs were observed in the treated samples. In this regard, P3D1 was the next effective crRNA and reduced viral RNA levels to ~45.4-fold in comparison to control.

Pooling and delivery of multiple crRNAs showed no significant effect on viral replication in all subtypes (Figures 3B, 3C, and 3D).

Comparison of silencing efficiency of Cas13 and RNAi

Some studies have used position-matched shRNAs to compare the silencing efficiency of CRISPR-Cas and RNAi systems.^{15,17,26,27} This means that the shRNAs are forced to be designed according to the position of crRNAs, which can affect the specificity and efficiency of shRNAs. However, CRISPR-Cas and RNAi systems can be compared under the same conditions, if shRNAs are designed efficiently based on the specific parameters that maximize the silencing potential of them. In the present study, position-matched shRNAs were not used and shRNAs were designed according to a scoring system that considers their specificity as well as silencing efficiency (materials and methods). To show the efficiency of CRISPR-Cas targeting to other established strategies that have demonstrated to be effective against viruses, plasmids expressing individual shRNAs, a cocktail of three shRNA-encoding plasmids targeting different genes or non-targeting shRNA control were transfected into the BHK-21 cells. Twenty-four hours after transfection, BHK-21 cells were challenged

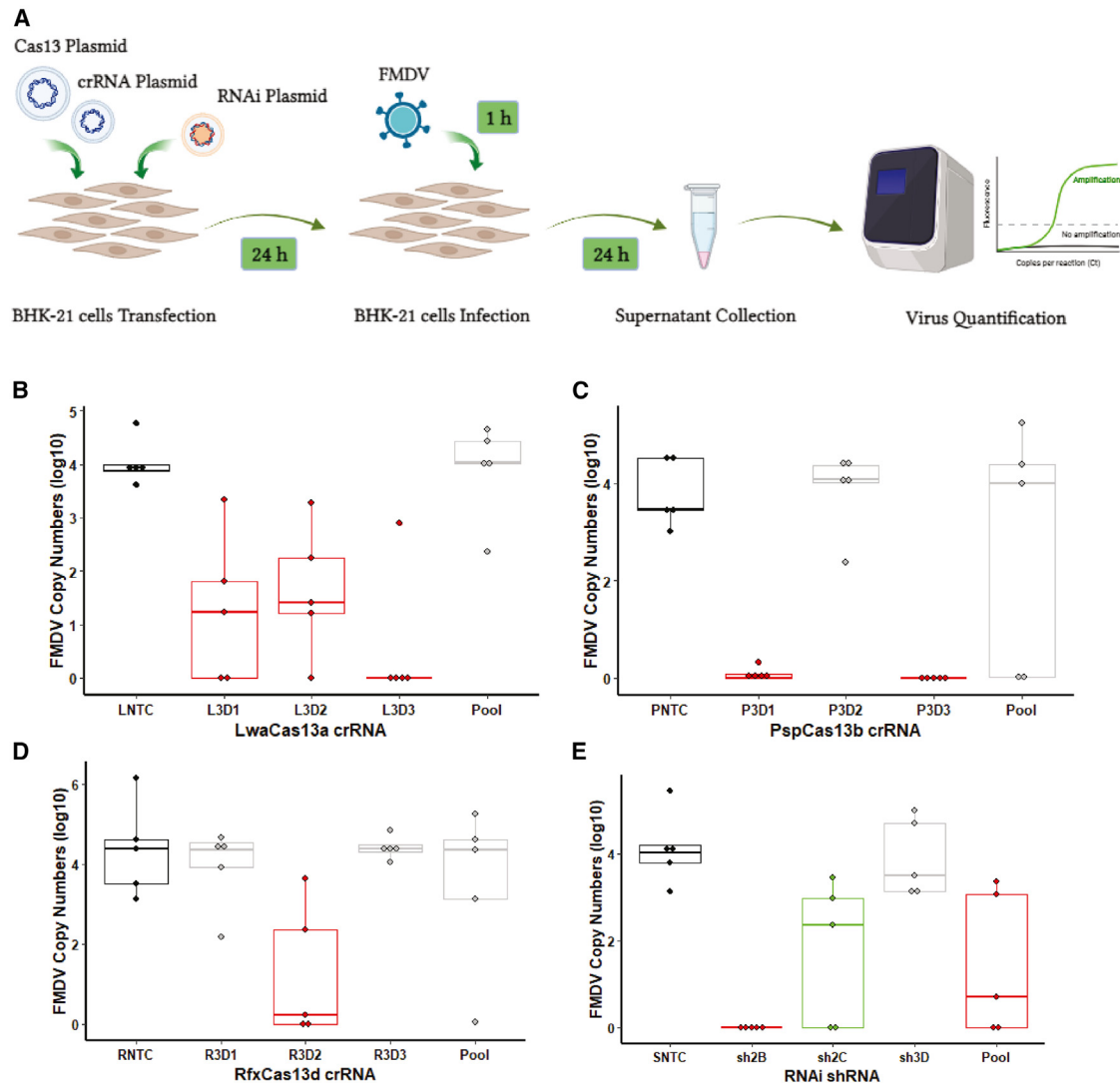


Figure 3. Effect of Cas13 and RNAi on FMDV inhibition, serotype O

(A) Experimental procedure for evaluating Cas13s and RNAi antiviral activity in BHK-21 cells. BHK-21 cells were transfected with plasmids containing targeting and non-targeting shRNAs or Cas13 and crRNAs that target or do not target FMDV 24 h before infection. Then the supernatants were collected 24 hpi to evaluate the antiviral activity. Silencing efficiency of *LwaCas13a* (B), *PspCas13b* (C), *RfxCas13d* (D), and RNAi system (E) on FMDV virus according to RT-qPCR results. In (B) to (E), data points in the graph are five independent biological experiments performed in technical replicates, lines indicate means; error bars represent SD; t test was performed to compare each treatment to non-targeting crRNA or shRNA (green and red color of the boxes indicate $p < 0.05$ and $p < 0.01$, respectively).

with FMDV serotype O and viral RNA levels in culture supernatant were quantified using RT-qPCR, 24 hpi. Suppression of viral RNAs was detected in the cells expressing sh2B and sh2C ($p < 0.0001$ and $p < 0.05$, respectively, Figure 3E). sh3D shRNA that was identified by i-Score and OligoWalk tools as well as obtained an acceptable score based on our scoring system, failed to repress FMDV, while was accidentally location-matched shRNA (Figure 2). Moreover, unlike CRISPR experiments, pooling different shRNAs designed for dissimilar genes was able to reduce viral replication ($p \leq 0.01$, Figure 3E). This result showed that RNAi-mediated knockdown is comparable to CRISPR-Cas.

crRNAs targeting efficiency against the diverse FMDV strains

The silencing efficiency of *LwaCas13a*, *PspCas13b*, and the RNAi system against another prevalent FMDV serotype, type A, was investigated to determine how well the crRNAs could target the diverse FMDV strains. Since L3D3, P3D3, and sh2B (Figures 3B, 3C, and 3E) showed higher efficiency than the other crRNAs or shRNAs, they were selected for this experiment. BHK-21 cells were transiently transfected with plasmids encoding *LwaCas13a* or *PspCas13b* and crRNA or shRNA-encoding plasmids. Twenty-four hours following transfection, cells were challenged by FMDV serotype A. Supernatant from infected cells was isolated 24 hpi and viral RNA abundance was

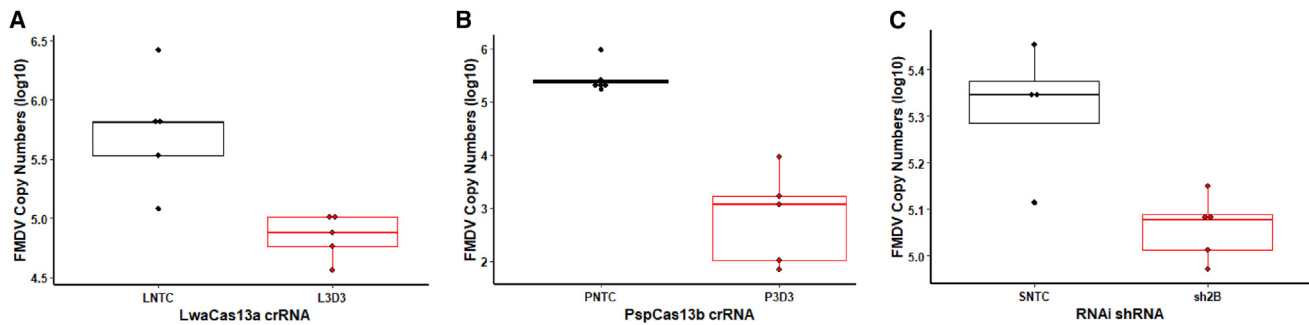


Figure 4. Effect of Cas13 and RNAi on FMDV inhibition, serotype A

Silencing efficiency of *LwaCas13a* (A), *PspCas13b* (B), and the RNAi system (C) on FMDV virus according to RT-qPCR results. In (A)–(C), data points in the graph are four or five independent biological experiments performed in technical replicates, lines indicate means; error bars represent SD; t test was performed to compare each treatment to non-targeting crRNA or shRNA (red color of the boxes indicates $p < 0.01$).

quantified by RT-qPCR. The results showed that both L3D3 and P3D3 crRNAs significantly reduced the viral RNA levels, in comparison with control ($p < 0.01$ and $p < 0.001$, respectively), demonstrating their efficiency to inhibit different FMD serotypes (Figures 4A and 4B). Consistent with the previous experiment, suppression of viral RNAs by these crRNAs is comparable to sh2B ($p < 0.01$, Figure 4C).

Evaluation of Cas13-mediated inhibition of infectious virions production

Although RT-qPCR is well established and widely used as the gold-standard method for viral copy number quantification, this approach cannot distinguish between partial genomic fragments (without infectivity) and intact genomes that can produce infectious virions.²⁸ Therefore, RT-qPCR may overestimate the number of infectious particles in the supernatant containing degraded and packaged genomic fragments, resulting from Cas13 activity. Hence, to illustrate the inhibitory effect of the CRISPR-Cas13 system on producing infectious particles, TCID50 assay was applied (Figure 5A). This method can overcome the drawbacks of RT-qPCR and measure sample infectivity. To do this, the remaining supernatants from the transfected cells with L3D2 crRNA in the *LwaCas13a* experiment (Figure 3B) and sh2C shRNA in the RNAi experiment (Figure 3E) were used in order to make a better comparison between the results of RT-qPCR and TCID50 assay. Results of this experiment revealed that *LwaCas13a* and RNAi knockdown activity reduced FMDV infectivity by ~ 7 - and ~ 56 -fold than control treatment, respectively (Figure 5B). This was while L3D2 and sh2C with the lowest viral inhibition among other crRNAs and shRNAs resulted in ~ 2.5 - and 2.3-fold reduction, respectively, in FMDV RNA levels as measured by RT-qPCR. Therefore, the Cas13-like RNAi system not only inhibited FMDV viral replication but also suppressed the formation of infectious virions. These results together demonstrate that animal ssRNA viruses can be targeted by Cas13 orthologs and may aid in the development of Cas13-based anti-FMDV therapeutics.

DISCUSSION

Emerging and reemerging animal and human viruses presented themselves as a perennial problem. Many animal viruses not only

infect different species but also have the potential to cause diseases in humans. Among all potential pathogens that may be involved in interspecies transmissions, RNA viruses are still the most important candidates for the next global zoonotic pandemic. Moreover, they play a major role in human and animal emerging pathogens.²⁹ Intense global mobility and increased human-animal interactions have created favorable conditions for animal viral transmission and posed an urgent need for tailor-made antivirals. Concerning this, repression of FMDV with diverse serotypes and many subtypes that geographically and genetically depict distinct evolutionary origins, is challenging. Conventional vaccines have serious limitations associated with FMD prevention, because the virus mutates rapidly and the vaccine needs to be updated regularly with new isolates from the field. In contrast, combination of more strains increases the cost of vaccine production and restricts its use in many developing countries.

CRISPR that is part of the bacteria and archaea immune system can be employed to combat foreign genetic elements.³⁰ Endonuclease activity of Cas13s has been repurposed for protection against animal and human viral pathogens. Here it was demonstrated that the CRISPR-Cas13 system has the potential to serve as an antiviral with common targets in various serotypes of highly pathogenic FMDV. In good agreement with the previous reports that demonstrated that viral enzymes targeting is one of the most effective methods in viral blockage (for several viruses like SARS-CoV-2, HIV, and HCV),^{31,32} our FMDV genome screening revealed that FMDV polymerase enzyme (*3D* gene) can be the most important target for antiviral development according to the CRISPR-Cas13 system. The CRISPR-Cas13 system is a promising antiviral strategy for FMDV, as it can specifically and efficiently target common regions of diverse and circulating strains, providing cross-protection across serotypes and rapid deployment. The CRISPR approach can take account of the characteristics of the different serotypes in different ecological systems by targeting conserved regions among all serotypes. In addition, Cas13s with targeting RNA instead of heritable DNA are considered safer versions of Cas enzymes.

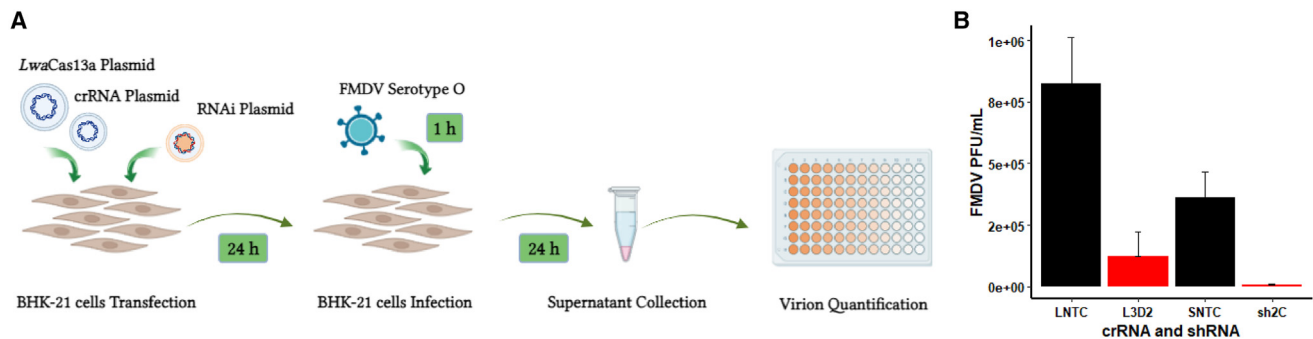


Figure 5. Effect of Cas13 and RNAi on FMDV infectivity

(A) Experimental schematic for evaluation of infectious particles production inhibition. BHK-21 cells were co-transfected with *LwaCas13a* and L3D2 or LNTC crRNA encoding plasmids or plasmids encoding sh2C and SNTC shRNA 24 h before infection with FMDV serotype O. Then the supernatants were collected 24 hpi to quantify infectious virions using TCID50 assay. (B) Representative data of the TCID50 assay. The number of infectious virions was expressed as FMDV plaque-forming units/mL (PFU/mL). In (B), lines indicate means; error bars represent SD; t test was performed to compare the two treatments (red color of the bar indicates $p < 0.01$).

Depending on the functionality that is needed for antiviral therapies, three groups of Cas13 orthologs were tested: Cas13a, Cas13b, and Cas13d. Unlike some other Cas13 effectors, *LwaCas13a* has more flexibility for therapeutic applications, as it can target any RNA genome that matches the crRNA, regardless of the adjacent nucleotide.¹⁶ The *PspCas13b* ortholog can be an alternative and appropriate choice, because of its increased specificity and long spacer sequence.³³ The small size and high catalytic activity of *RfxCas13d* makes it a promising application prospect in this field.¹⁸ As expected, some of the designed crRNAs failed to inhibit the infection and did not yield optimal silencing, which emphasized that Cas13 knockdown activity depends on multiple parameters, some of which remain unclear. Thus, experimental validation of the designed crRNAs is necessary. In spite of the various silencing efficiency, all the investigated Cas13 orthologs were able to cleave FMDV RNA and efficiently suppress viral replication in cell culture. Furthermore, the TCID50 assay revealed that this efficiency can be underestimated, as RT-qPCR overestimates RNA copy numbers of functional viruses. Hence, it is expected to have a higher silencing efficiency of Cas13s in practice.

Multiplexing based on tiled crRNAs in the present study yielded unsatisfactory results. This finding can be justified by taking into account the target accessibility due to excessive accumulation of Cas13-crRNA complexes in one region. Moreover, crRNAs can compete and interfere with each other, preventing them from forming functional complexes with Cas proteins. It worth noting that we were forced to design the crRNAs in a limited conserved region (Figure 2). All in all, these negative effects can affect the efficiency and kinetics of the CRISPR-Cas system³⁴ and pointed out that multiplexing does not necessarily outperform a single crRNA. This is in complete agreement with the Fareh et al. study that tested pooled crRNAs against SARS-CoV-2 and obtained no better results than single crRNA to enhance viral suppression. In another study by Freije et al., a modestly increased effect was obtained by pooling four crRNAs against IAV.^{17,33} Hence, possible drawbacks and challenges need to be considered in using multiplexing of crRNAs. For example, it would

be better to design crRNAs targeting different regions to prevent crRNA competition and provide target accessibility for each crRNA.

Defense against invading pathogens can be achieved by powerful approaches like CRISPR-Cas13 and RNAi and both methods are mediated by small noncoding RNAs that guide a ribonucleoprotein complex toward the targets. Therefore, the first step to make a precise comparison between silencing efficiency of these approaches is designing efficient crRNAs/shRNAs. In spite of the availability of efficient crRNA designing tools such as CaSilico, there is not an appropriate tool that considers comprehensive and up-to-date rules to design specific and effective shRNAs.³⁵ It is worth highlighting that in the present study a scoring system was developed to prioritize the designed shRNAs by different tools. We considered 29 rules based on the previous reports,^{36–38} which include the important features for an efficient shRNA. This scoring system provides a resource for the researchers to evaluate their shRNAs and choose the accurate ones. Taking into account designing efficient crRNAs/shRNAs, the silencing efficiency of CRISPR-Cas13 and RNAi methods were compared and the results revealed that the potential of CRISPR and RNAi in FMDV knockdown were the same. Although both methods target RNA molecules, the CRISPR-Cas13 system has some advantages over RNAi. CRISPR-Cas13 shows higher specificity than RNAi, since perfect base pairing between crRNA and the target is needed for activation of the Cas effector, and some subtypes such as Cas13b must recognize a PFS (protospacer flanking site) for RNA cleavage to occur. RNAi on the other hand, lacks exclusive RNA targeting and works even with partial base pairing between guide and the target, suffering from more off-target effects.³⁹ Some viruses have evolved strategies to impair cellular RNAi pathways, in this situation the CRISPR-Cas system as an RNAi machinery-independent strategy can effectively degrade viral genomes.⁴⁰ In addition, unlike RNAi, which can only target cytoplasmic transcripts, Cas13 can also target nuclear transcripts. Using CRISPR-Cas13-based technologies will require efficient administration of CRISPR-Cas components into target cells, a major technical issue that has hindered the

widespread application of CRISPR-based therapeutics and limits CRISPR applications in clinical settings.⁴¹ Recent advances like virus-like particles, mRNA-based platforms, nanocomposites, and molecular adjuvants have tried to overcome this challenge.^{42,43}

Since FMDV has a short reproductive cycle with factors that promote viral multiplication in host cells,⁴⁴ timely suppression of a virulent virus highlights the power of the CRISPR-Cas13 system as a novel antiviral approach. Our results demonstrated the potential of CRISPR-Cas13-based antivirals to broadly target many serotypes of FMDV viruses, which reinforced their therapeutic importance in veterinary medicine. Animal protection using development of CRISPR-Cas antivirals can be developed faster than for humans, as the regulatory approval process is less strict for animal use. Hence, developing CRISPR-based viral suppressors that inhibit different serotypes, by targeting conserved regions, can be a huge barrier against viral evolution and will be effective against future mutant viruses. With a safe and effective delivery system, our method has the potential to be an important FMDV inhibition strategy. Moreover, this approach is easily expandable to other pathogenic viruses besides FMDV, which makes it a unique strategy for antiviral therapeutics.

MATERIALS AND METHODS

Genome sequences collection

Complete genome sequences of representative strains or isolates (where available) belong to FMDV topotypes derived from serotypes O, A, C, Asia 1, SAT 1, SAT 2, and SAT 3 that were obtained from the website of Pirbright Institute (<https://www.wrlfmd.org>). Representative strains capture the genetic diversity of all FMDV serotypes, as they show a high degree of variability. The multiple sequence alignment (MSA) for 1D gene sequences of representative strains was done using the MAFFT (v7.475) tool, default settings with progressive method (FFT-NS-2). A phylogenetic tree and the associated annotations based on the MSA result were constructed by the neighbor-joining method and jukes-cantor model. Finally, the Interactive Tree Of Life (iTOL, v6) platform⁴⁵ was used for further phylogenetic tree visualization and annotation (supplemental information, Figure S1; Table S2).

crRNA design

To design crRNAs that target simultaneously various strains of FMDV, first, the most conserved genes among the strains were detected. To do this, annotation of the complete genomic sequences of FMD representative strains was performed based on the reference genome of FMDV (accession number NC039210, from NCBI database). MSA for each class of the genes was conducted using the MAFFT (v7.475) tool, default settings with progressive method (FFT-NS-2).⁴⁶ The results were further investigated through the SIAS online tool (<http://imed.med.ucm.es/Tools/sias.html>) to identify gene identity or homology percentages. In this step, we selected three genes with the highest degree of similarity among the strains for further analysis. Then, the sequences of each selected gene from the genome of strains were extracted and subjected to crRNA designing using our CaSilico R package, to design crRNAs for class

II of the CRISPR system (type VI-A/B/D). Taking into account a list of important features such as mismatch tolerance rules, frequency of cleaving base around the target site, target accessibility, self-complementarity, GC content, PFS requirement, and off-target analysis, CaSilico searches all potential crRNAs in a user-input sequence and ranks them according to these features.¹⁹ Moreover, as a unique feature of CaSilico, it can automatically design crRNAs that simultaneously target multiple sequences through conserved region detection among the sequences. This feature enabled us to design crRNAs that simultaneously target each gene in different strains. Non-targeting crRNA control (NTC) for each subtype was created by shuffling the nucleotide sequence of one 3D targeting candidate crRNA in that subtype. NTCs were assessed for self-complementarity and GC content and BLASTn tool (with word size = 7 and an E-value = 10 cutoff) was employed to identify potential off-targets against FMDV genomes as well as bovine, ovine, caprine, and porcine transcriptome.

shRNA design

To improve the shRNA efficiency, seven of the most popular designing tools (siDirect, i-Score, s-Biopredsi, DSIR, Oligowalk, RNAXs, BLOCK-iT RNAi designer) were applied. As described above, three of most conserved genes among the strains were detected and a consensus sequence for each gene was generated by EMBOSS tool (https://www.ebi.ac.uk/Tools/msa/emboss_cons/). The consensus sequences were inputted into the shRNA designing tools. Then, the candidate shRNAs were filtered according to a self-developed filtering system that considers some important parameters such as specific positional rules, nucleotide composition rules, thermodynamics rules, and off-target analysis (Table 2). BLASTn tool (with word size = 7 and an E-value = 10 cutoff) was employed to identify potential off-target hits against bovine, ovine, caprine and porcine transcriptome. The hits with a coverage of at least 78% with unrelated RNA targets were considered as off-targets. The candidates with off-targets were not considered for further evaluation according to our scoring system. The other specific candidates were evaluated and a score was assigned to each shRNA according to the 29 various characteristics (Table 2), as higher scores indicate the higher efficiency. Non-targeting shRNA control (NTC) was also created by shuffling the nucleotide sequence of 2B targeting shRNA (sh2B) and was assessed according to the filtering system. Non-targeting control was blasted against FMDV genomes as well as bovine, ovine, caprine, and porcine transcriptome.

Cloning of FMDV-targeting crRNAs and shRNAs

To generate crRNAs and shRNAs, spacers, shRNAs, and their reverse complementary DNA oligomers were synthesized as single-stranded DNA (ssDNA) by GenScript Biotech. Spacers were cloned into pC0040-*Lwa*Cas13a, pC0043-*Psp*Cas13b, or pXR003-*Rfx*Cas13d guide RNA expression backbone plasmids (Addgene #103851, #103854, and #109053, respectively) and shRNAs were cloned into pMKO.1 puro plasmid (Addgene #8452). For spacer cloning in these vectors, the double BbsI restriction site is present upstream of *Lwa*-Cas13a and *Rfx*Cas13d crRNA direct repeat (DR) sequence or

Table 2. Scoring system for predicting siRNA efficiency using various characteristics

NO	Parameters	Score
Specific Positional Rules^{37,38,47-53}		
1	Weak base pairing at 5' end of antisense strand (presence of A/U at first position of antisense strand) ^a	2
2	Strong base pairing at 5' end of sense strand (presence of G/C at first position of sense strand) ^b	2
3	Presence of A and absence of C at the third position of sense strand	2
4	Absence of C at the fifth position of sense strand	1
5	Presence of A/U at the sixth position of sense strand	1
6	Absence of C at the seventh position of sense strand	1
7	Presence of U at the eighth position of sense strand	1
8	Presence of A/U and absence of C at 10 th position of sense strand ^c	2
9	Absence of G at 11 th position of sense strand	1
10	Absence of G at 13 th position of sense strand	1
11	Absence of G at 14 th position of sense strand	1
12	Presence of A/C at 16 th position of sense strand	1
13	Absence of G at 17 th position of sense strand	1
14	Presence of A at 6 th position of antisense strand	1
15	Presence of U and absence of C at 7 th position of antisense strand	2
16	Presence of A at 10 th position of antisense strand	1
17	Presence of U and absence of G at 13 th position of antisense strand	2
18	Presence of U and absence of G at 14 th position of antisense strand	2
19	Absence of A at 17 th position of antisense strand	1
Nucleotide Composition Rules^{47,48,54}		
20	At least 3 A/U bases between 13 th and 19 th position (seed region) of sense strand ^d	2
21	Less than 4 consecutive G/C and A/T ^e	1
22	Having GC content of 36%–52%	1
23	Having energy valley in 9 th –14 th position of the sense strand (lower GC content) ^f	2
24	Perfect base pairing with target region (mismatch at 5' or 3' ends can be tolerated) ^g	2
Thermodynamics Rules⁵⁵		
25	Low T _m at seed region (2–7 nt) of antisense strand ^h	2
26	The ΔG value throughout the siRNA stretch <34 (–kcal/mol)	2
27	Not having any stable internal secondary structures ⁱ	2
Blast Rules		
28	BLAST of seed region	2
29	BLAST of sense or antisense strand	2

^aBases A and U are preferred within seven bases toward the 5' end.
^bRNA polymerase III initiates transcription more efficiently when one purine is present at the 5'-end of the sense strand.
^cRISC similar to most endonucleases cleaves mRNA between nucleotide 10 and 11 and prefers 3' of U.
^dThis is important for target specificity and stability of the siRNA-mRNA duplex.
^eRNA polymerase III often ends transcription at the poly A site.
^fEnergy valley boosts the complexity of RISC by prompting the most desirable conformation during mRNA cleavage.
^gsiRNAs recognize their target by perfect base pairing in positions 2–7 of the guide strand, which is known as the seed region, allowing bulges and loops in another region of the duplex. Few mismatches, particularly near the end of the duplex, partially reduce the rate and extent of cleavage.
^hIn order to ensure a functional siRNA with minimized off-target effects, the melting temperature of the seed duplex must be less than 21.5°C.
ⁱSecondary structures with T_m values less than 33°C can be tolerated since they are unwound by body temperature, 37°C.

downstream of *PspCas13b* DR nucleotides. A total of 1 μ g CRISPR and RNAi plasmids were linearized by *BbsI* digestion (Thermo Fisher Scientific) and *EcoRI*-*AgeI* (Thermo Fisher Scientific) double digestion following the manufacturer's instructions (1 h at 37°C), respectively. NEBcutter (v3.0.17) was used to check if there are any restriction enzyme sites inside the spacers and shRNAs sequences. The enzymatic digestion was verified by 1% agarose gel. Complementary oligos for each spacer or shRNA at 10 μ M were annealed in annealing buffer (10 mM Tris at pH 7.5–8.0, 50 mM NaCl, 1 mM EDTA) in the presence of T4 PNK (NEB). The tubes were incubated at 37°C for 30 min, then at 95°C for 5 min followed by a ramp from 95°C to 4°C at a rate of 1°C/min in the thermocycler. The annealed oligos were diluted 1:10 and then ligated into the digested vectors using T4 DNA Ligase (Thermo Fisher Scientific, 1 h at 37°C).

Plasmid amplification and purification

The ligated plasmids were transformed into chemically competent bacteria (DH5 α) using the heat shock method and plated for transformants on lysogeny broth (LB) agar plates containing ampicillin at 37°C overnight. Colony PCR and Sanger sequencing were performed to screen and verify recombinant clones. Single positive colonies were picked and inoculated into LB agar cultures supplemented with ampicillin and incubated 16 h for miniprep purification. Plasmid DNA was extracted using Monarch Plasmid Miniprep Kit (NEB) according to the manufacturer's instructions and stored at –20°C. Plasmids encoding Cas13 effectors available at Addgene (pC0056 #105815, pC0046 #103862, and pXR001 #109049) were transformed and isolated with the same protocol used for backbone plasmids described above.

Cell culture

Baby hamster kidney cells (BHK-21, ATCC) were used to prepare FMD virus stocks and determine virus titers, evaluate Cas13 activity against FMDV, and perform the virus infectivity experiment. Low-passage-number cells that were free of mycoplasma contamination were used. We checked for mycoplasma with PCR using two sets of primers that targeted the 16S rRNA gene, which is highly conserved among different mycoplasma species. These primers did not amplify eukaryotic DNA or bacteria that are closely related to mycoplasma (fwd1: TGGGGAGCAAACAGGATTAGATACC; rev1: TGCACCA TCTGTCACTCTGTAAACCTC, fwd2: GCTGCGGTGAATAC GTTCT; rev2: TCCCCACGTTCTCGTAGGG ordered from GenScript Biotech). The amplification cycling was as follows: initial denaturation at 95°C for 5 min, followed by 40 cycles of 94°C for 30 s, 54 for 30 s, and 72°C for 60 s, and a final extension for 10 min at 72°C.

BHK-21 cells were cultured in Dulbecco's Modified Eagle Medium (DMEM) with high glucose, GlutaMAX, 25 mM HEPES, sodium pyruvate (Thermo Fisher Scientific) containing 10% heat inactivated fetal bovine serum (FBS) (Thermo Fisher Scientific), penicillin-streptomycin (Thermo Fisher Scientific) (cDMEM-10% FBS). Cell lines were incubated in tissue culture incubators at 37°C and 5% CO₂.

FMDV propagation and titrating

BHK-21 cells were grown until complete and confluent monolayer in 25-cm² culture flasks. To propagate FMDV stock, growth media was removed and cells were washed twice with PBS. Then, cells were infected at an MOI of 0.2 PFU per cell for 1.5 h in serum-free media. For better absorption, culture flasks were rocked manually every 15 min to spread inoculum over the cell sheet. The cDMEM-2% FBS was added to the cells after 1.5 h and they were returned to the incubator and kept at 37°C. Cells were monitored for 48 h under an inverted microscope until the development of characteristic cytopathic effect (CPE). Viral culture supernatant was harvested after observing severe CPE. To remove cell debris, infectious fluid was pooled and centrifuged at 1,000 \times g for 10 min. The resulting stock was aliquoted and stored at –80°C for later use.

FMDV infectivity assay

Infectivity titers of viral stocks were determined using the median tissue culture infectious dose (TCID₅₀) method.⁵⁶ For titration, confluent cell monolayers were trypsinized, counted, and resuspended in cDMEM-6% FBS. Then, 50 μ L of cell suspension containing 5 \times 10⁴ cells was put in each well of 96-well plates (Orange Scientific). Ten-fold serial dilutions of viral stock with one freeze-thaw cycle prepared in serum-free cDMEM so that dilution range was from 10^{–1} to 10^{–10} and 100 μ L of each dilution was added to the wells of 96-well plates, eight replicates per dilution. As controls, first and second columns were left without virus and 100 μ L of serum-free cDMEM was put in them instead. Cells were incubated for 3 days at 37°C with 5% CO₂ and checked daily for presence or absence of CPE using an inverted microscope. The endpoint titers were calculated by means of the Reed & Muench method and expressed as TCID₅₀/mL.

Plasmid DNA transfection and viral infection

All transfection experiments were performed in 96-well tissue culture-treated flat-bottom plates (Orange Scientific) using Lipofectamine 2000 (Thermo Fisher Scientific). Confluent BHK-21 cells were trypsinized and counted to estimate cell density. Since all transfections were performed prior to infections, 3.5 \times 10⁴ cells per well were seeded 24 h before transfection to ensure 90%–95% confluency at the time of transfection. In VI-A CRISPR-Cas experiments, BHK-21 cells were transfected per well with 150 ng of plasmids encoding *LwaCas13a* and 200 ng of crRNA-encoding plasmids or non-targeting crRNA plasmid. In VI-B and VI-D CRISPR-Cas experiments 100 and 200 ng of plasmids encoding *PspCas13b* and *RfxCas13d* and 150 and 200 ng of crRNA-encoding plasmids or non-targeting crRNA plasmid were used, respectively. For each well, plasmids were combined with Opti-MEM I Reduced Serum Medium (Thermo Fisher Scientific) to a total of 25 μ L. In a separate tube, 0.9 μ L of Lipofectamine 2000 was mixed with 24.1 μ L of Opti-MEM. Solution 1 and solution 2 were added together, mixed completely, and incubated at room temperature for 20 min. The growth medium was gently aspirated from the cells and 110 μ L of cDMEM-2% FBS (without antibiotic) was added to each well. Then, the transfection complex was slowly pipetted onto cells. Transfection conditions for shRNA

experiments were the same as explained above, except 250 ng of shRNA-encoding plasmids or non-targeting shRNA plasmid were transfected per well. After transfection, cells were incubated at 37°C with 5% CO₂.

FMDV infection

Twenty-four hours post transfection (hpt), transfection complex was removed and cells were washed twice with DMEM. Cells were infected with 100 µL of FMDV at 10³ TCID₅₀/mL (viral stock was diluted in serum-free cDMEM) for 1 h with plate shaken manually every 15 min. To remove excess virus and measure newly produced viral RNA, inoculant was removed after 1 h of adsorption and cells were washed twice with DMEM. The infection proceeded in cDMEM-2% FBS, then virus containing cellular supernatants was harvested 24 h post infection (hpi) and stored at –80°C for further analysis.

Viral RNA quantification in supernatant

FMDV that could replicate and infect cells was quantified by RT-qPCR assay. In order to construct the standard curve for quantification of viral load, 10-fold serial dilutions of FMDV PCR target fragments from 10⁹ to 10 copies per microliter were used. Three separate dilution series were prepared, and each dilution within each series was amplified in duplicate. Viral RNA was extracted from harvested supernatant of infected cells using the QIAamp viral RNA mini kit (Qiagen) with carrier RNA following the manufacturer's instructions and stored at –80°C until use. 3D region primer set was ordered from GenScript Biotech (forward: CTCTCCTTGCACGCCGTG; reverse: CGCAGGTAAAGTGATCTGTAGCT) and RT-qPCR was conducted by BlazeTaq One-Step SYBR Green RT-qPCR kit (Genecopoeia) on a Rotor-Gene Q instrument (Qiagen) in accordance with the manufacturer's instructions. The cycling parameters were 42°C for 10 min for reverse transcription, and then 95°C for 3 min followed by 40 cycles of 95°C for 15 s and 69°C for 30 s. Two technical replicates for each sample were considered and a melt curve analysis was produced to confirm specificity of the amplified product.

To monitor infectious virions, 24 hpi viral culture supernatant was removed from BHK-21 expressing *LwaCas13a*, L3D2, and LNTC crRNA or sh2C and SNTC shRNA. Samples were pooled across the biological replicates. TCID₅₀ assay was performed in triplicate as described above in “FMDV infectivity assay.”

Statistical analysis

In each transfection experiment, five biological replicates were used. For RT-qPCR analysis, the standard curve was used to convert Ct values into the viral RNA copy numbers. Copy number for each biological replicate was calculated using the average of the duplicate cycle threshold values. In all experiments, data analysis and plotting were performed in R software. Unpaired two-tailed Student's t test was used to calculate *p* values and compare the statistical significance between targeting and non-targeting groups. A *p* value less than 0.05 was considered statistically significant.

DATA AND CODE AVAILABILITY

All datasets and codes are available upon reasonable request.

SUPPLEMENTAL INFORMATION

Supplemental information can be found online at <https://doi.org/10.1016/j.omtn.2024.102235>.

ACKNOWLEDGMENTS

The authors would like to acknowledge the financial support of INFS (Iran National Science Foundation; grant 99004902) for this research.

AUTHOR CONTRIBUTIONS

A.A. conceived and designed the study under the guidance and supervision of M.R.B., M.S., and M.H.M. A.A. conducted all sections of experiments and data analysis. N.S. and Z.Z.K. assisted in cell culture, FMDV propagation and titrating, and FMDV infectivity assay. H.F. and A.G. and H.E. provided critical insights on protocols, the results, and the work. A.A. wrote the paper with guidance from M.R.B. M.R.B. and H.F. discussed the results and commented on the manuscript. M.R.B. reviewed the manuscript.

DECLARATION OF INTERESTS

All authors declare no competing interests.

REFERENCES

- Kausar, S., Said Khan, F., Ishaq Mujeeb Ur Rehman, M., Akram, M., Riaz, M., Rasool, G., Hamid Khan, A., Saleem, I., Shamim, S., and Malik, A. (2021). A review: Mechanism of action of antiviral drugs. *Int. J. Immunopathol. Pharmacol.* 35, 20587384211002621. <https://doi.org/10.1177/20587384211002621>.
- Singh, M., and de Wit, E. (2022). Antiviral agents for the treatment of COVID-19: Progress and challenges. *Cell Rep. Med.* 3, 100549. <https://doi.org/10.1016/j.xcrm.2022.100549>.
- Grubman, M.J., and Baxt, B. (2004). Foot-and-Mouth Disease. *Clin. Microbiol. Rev.* 17, 465–493. <https://doi.org/10.1128/CMR.17.2.465-493.2004>.
- Knight-Jones, T.J.D., and Rushton, J. (2013). The economic impacts of foot and mouth disease – What are they, how big are they and where do they occur? *Prev. Vet. Med.* 112, 161–173. <https://doi.org/10.1016/j.prevetmed.2013.07.013>.
- Tomar, S., Mahajan, S., and Kumar, R. (2020). Advances in structure-assisted antiviral discovery for animal viral diseases. In *Genomics and Biotechnological Advances in Veterinary, Poultry, and Fisheries* (Elsevier), pp. 435–468. <https://doi.org/10.1016/B978-0-12-816352-8.00019-9>.
- Pattnaik, B., Subramaniam, S., Sanyal, A., Mohapatra, J.K., Dash, B.B., Ranjan, R., and Rout, M. (2012). Foot-and-mouth Disease: Global Status and Future Road Map for Control and Prevention in India. *Agric. Res.* 1, 132–147. <https://doi.org/10.1007/s40003-012-0012-z>.
- Parida, S. (2009). Vaccination against foot-and-mouth disease virus: strategies and effectiveness. *Expert Rev. Vaccines* 8, 347–365. <https://doi.org/10.1586/14760584.3.347>.
- NIEDBALSKI, W., FITZNER, A., and BULENGER, K. (2019). Recent progress in vaccines against foot-and-mouth disease. *Med. Weter.* 75, 6212. <https://doi.org/10.21521/mw.6212>.
- Kamel, M., El-Sayed, A., and Castañeda Vazquez, H. (2019). Foot-and-mouth disease vaccines: recent updates and future perspectives. *Arch. Virol.* 164, 1501–1513. <https://doi.org/10.1007/s00705-019-04216-x>.
- Hardham, J.M., Krug, P., Pacheco, J.M., Thompson, J., Dominowski, P., Moulin, V., Gay, C.G., Rodriguez, L.L., and Rieder, E. (2020). Novel Foot-and-Mouth Disease Vaccine Platform: Formulations for Safe and DIVA-Compatible FMD Vaccines

- With Improved Potency. *Front. Vet. Sci.* 7, 554305. <https://doi.org/10.3389/fvets.2020.554305>.
11. Rodriguez, L.L., and Gay, C.G. (2011). Development of vaccines toward the global control and eradication of foot-and-mouth disease. *Expert Rev. Vaccines* 10, 377–387. <https://doi.org/10.1586/erv.11.4>.
 12. Puckette, M., Clark, B.A., Barrera, J., Neilan, J.G., and Rasmussen, M.V. (2023). Evaluation of DNA Vaccine Candidates against Foot-and-Mouth Disease Virus in Cattle. *Vaccines* 11, 386. <https://doi.org/10.3390/vaccines11020386>.
 13. Mignauqui, A.C., Ruiz, V., Durocher, Y., and Wigdorovitz, A. (2019). Advances in novel vaccines for foot and mouth disease: focus on recombinant empty capsids. *Crit. Rev. Biotechnol.* 39, 306–320. <https://doi.org/10.1080/07388551.2018.1554619>.
 14. Lu, Z., Yu, S., Wang, W., Chen, W., Wang, X., Wu, K., Li, X., Fan, S., Ding, H., Yi, L., et al. (2022). Development of Foot-and-Mouth Disease Vaccines in Recent Years. *Vaccines* 10, 1817. <https://doi.org/10.3390/vaccines10111817>.
 15. Abudayyeh, O.O., Gootenberg, J.S., Essletzbichler, P., Han, S., Joung, J., Belanto, J.J., Verdine, V., Cox, D.B.T., Kellner, M.J., Regev, A., et al. (2017). RNA targeting with CRISPR–Cas13. *Nature* 550, 280–284. <https://doi.org/10.1038/nature24049>.
 16. Li, H., Wang, S., Dong, X., Li, Q., Li, M., Li, J., Guo, Y., Jin, X., Zhou, Y., Song, H., et al. (2020). CRISPR–Cas13a Cleavage of Dengue Virus NS3 Gene Efficiently Inhibits Viral Replication. *Mol. Ther. Nucleic Acids* 19, 1460–1469. <https://doi.org/10.1016/j.omtn.2020.01.028>.
 17. Freije, C.A., Myhrvold, C., Boehm, C.K., Lin, A.E., Welch, N.L., Carter, A., Metsky, H.C., Luo, C.Y., Abudayyeh, O.O., Gootenberg, J.S., et al. (2019). Programmable Inhibition and Detection of RNA Viruses Using Cas13. *Mol. Cell* 76, 826–837.e11. <https://doi.org/10.1016/j.molcel.2019.09.013>.
 18. Abbott, T.R., Dhamdhare, G., Liu, Y., Lin, X., Goudy, L., Zeng, L., Chemparathy, A., Chmura, S., Heaton, N.S., Debs, R., et al. (2020). Development of CRISPR as an Antiviral Strategy to Combat SARS–CoV–2 and Influenza. *Cell* 181, 865–876.e12. <https://doi.org/10.1016/j.cell.2020.04.020>.
 19. Asadbeigi, A., Norouzi, M., Vafaei Sadi, M.S., Saffari, M., and Bakhtiarzadeh, M.R. (2022). Casilico: A versatile CRISPR package for in silico CRISPR RNA designing for Cas12, Cas13, and Cas14. *Front. Bioeng. Biotechnol.* 10, 957131. <https://doi.org/10.3389/fbioe.2022.957131>.
 20. Konermann, S., Lotfy, P., Brideau, N.J., Oki, J., Shokhirev, M.N., and Hsu, P.D. (2018). Transcriptome Engineering with RNA-Targeting Type VI-D CRISPR Effectors. *Cell* 173, 665–676.e14. <https://doi.org/10.1016/j.cell.2018.02.033>.
 21. Cox, D.B.T., Gootenberg, J.S., Abudayyeh, O.O., Franklin, B., Kellner, M.J., Joung, J., and Zhang, F. (2017). RNA editing with CRISPR–Cas13. *Science* 358, 1019–1027. <https://doi.org/10.1126/science.aag0180>.
 22. Shah, P.S., Pham, N.P., and Schaffer, D.V. (2012). HIV Develops Indirect Cross-resistance to Combinatorial RNAi Targeting Two Distinct and Spatially Distant Sites. *Mol. Ther.* 20, 840–848. <https://doi.org/10.1038/mt.2012.3>.
 23. Patel, H., and Kukol, A. (2017). Evolutionary conservation of influenza A PB2 sequences reveals potential target sites for small molecule inhibitors. *Virology* 509, 112–120. <https://doi.org/10.1016/j.virol.2017.06.009>.
 24. Gao, Y., Sun, S.-Q., and Guo, H.-C. (2016). Biological function of Foot-and-mouth disease virus non-structural proteins and non-coding elements. *Viol. J.* 13, 107. <https://doi.org/10.1186/s12985-016-0561-z>.
 25. Belsham, G.J. (2020). Towards improvements in foot-and-mouth disease vaccine performance. *Acta Vet. Scand.* 62, 20. <https://doi.org/10.1186/s13028-020-00519-1>.
 26. Sandoval, A., Elahi, H., and Ploski, J.E. (2020). Genetically Engineering the Nervous System with CRISPR–Cas. *eneuro* 7, ENEURO.0419-19.2020. <https://doi.org/10.1523/ENEURO.0419-19.2020>.
 27. Li, S., Li, X., Xue, W., Zhang, L., Yang, L.-Z., Cao, S.-M., Lei, Y.-N., Liu, C.-X., Guo, S.-K., Shan, L., et al. (2021). Screening for functional circular RNAs using the CRISPR–Cas13 system. *Nat. Methods* 18, 51–59. <https://doi.org/10.1038/s41592-020-01011-4>.
 28. Adamski, M.G., Gumann, P., and Baird, A.E. (2014). A Method for Quantitative Analysis of Standard and High-Throughput qPCR Expression Data Based on Input Sample Quantity. *PLoS One* 9, e103917. <https://doi.org/10.1371/journal.pone.0103917>.
 29. Carrasco-Hernandez, R., Jácome, R., López Vidal, Y., and Ponce de León, S. (2017). Are RNA Viruses Candidate Agents for the Next Global Pandemic? A Review. *ILAR J.* 58, 343–358. <https://doi.org/10.1093/ilar/ilx026>.
 30. Horvath, P., and Barrangou, R. (2010). CRISPR/Cas, the Immune System of Bacteria and Archaea. *Science* 327, 167–170. <https://doi.org/10.1126/science.1179555>.
 31. Peng, S., Wang, H., Wang, Z., and Wang, Q. (2022). Progression of Antiviral Agents Targeting Viral Polymerases. *Molecules* 27, 7370. <https://doi.org/10.3390/molecules27217370>.
 32. Adamson, C.S., Chibale, K., Goss, R.J.M., Jaspars, M., Newman, D.J., and Dorrington, R.A. (2021). Antiviral drug discovery: preparing for the next pandemic. *Chem. Soc. Rev.* 50, 3647–3655. <https://doi.org/10.1039/D0CS01118E>.
 33. Fareh, M., Zhao, W., Hu, W., Casan, J.M.L., Kumar, A., Symons, J., Zerbato, J.M., Fong, D., Voskoboinik, I., Ekert, P.G., et al. (2021). Reprogrammed CRISPR–Cas13b suppresses SARS–CoV–2 replication and circumvents its mutational escape through mismatch tolerance. *Nat. Commun.* 12, 4270. <https://doi.org/10.1038/s41467-021-24577-9>.
 34. Alok, A., Sandhya, D., Jogam, P., Rodrigues, V., Bhati, K.K., Sharma, H., and Kumar, J. (2020). The Rise of the CRISPR/Cpf1 System for Efficient Genome Editing in Plants. *Front. Plant Sci.* 11, 264. <https://doi.org/10.3389/fpls.2020.00264>.
 35. S. Hameed, and S. Rehman, eds. (2022). *Nanotechnology for Infectious Diseases* (Springer). <https://doi.org/10.1007/978-981-16-9190-4>.
 36. Fakhr, E., Zare, F., and Teimoori-Toolabi, L. (2016). Precise and efficient siRNA design: a key point in competent gene silencing. *Cancer Gene Ther.* 23, 73–82. <https://doi.org/10.1038/cgt.2016.4>.
 37. Ui-Tei, K., Naito, Y., Takahashi, F., Haraguchi, T., Ohki-Hamazaki, H., Juni, A., Ueda, R., and Saigo, K. (2004). Guidelines for the selection of highly effective siRNA sequences for mammalian and chick RNA interference. *Nucleic Acids Res.* 32, 936–948. <https://doi.org/10.1093/nar/gkh247>.
 38. Amarzgueni, M., and Prydz, H. (2004). An algorithm for selection of functional siRNA sequences. *Biochem. Biophys. Res. Commun.* 316, 1050–1058. <https://doi.org/10.1016/j.bbrc.2004.02.157>.
 39. Bartoszewski, R., and Sikorski, A.F. (2019). Editorial focus: understanding off-target effects as the key to successful RNAi therapy. *Cell. Mol. Biol. Lett.* 24, 69. <https://doi.org/10.1186/s11658-019-0196-3>.
 40. Yin, L., Zhao, F., Sun, H., Wang, Z., Huang, Y., Zhu, W., Xu, F., Mei, S., Liu, X., Zhang, D., et al. (2020). CRISPR–Cas13a Inhibits HIV-1 Infection. *Mol. Ther. Nucleic Acids* 21, 147–155. <https://doi.org/10.1016/j.omtn.2020.05.030>.
 41. Xu, C.-F., Chen, G.-J., Luo, Y.-L., Zhang, Y., Zhao, G., Lu, Z.-D., Czarna, A., Gu, Z., and Wang, J. (2021). Rational designs of in vivo CRISPR–Cas delivery systems. *Adv. Drug Deliv. Rev.* 168, 3–29. <https://doi.org/10.1016/j.addr.2019.11.005>.
 42. Ghani, M.W., Iqbal, A., Ghani, H., Bibi, S., Wang, Z., and Pei, R. (2023). Recent advances in nanocomposite-based delivery systems for targeted CRISPR/Cas delivery and therapeutic genetic manipulation. *J. Mater. Chem. B* 11, 5251–5271. <https://doi.org/10.1039/D2TB02610D>.
 43. Behr, M., Zhou, J., Xu, B., and Zhang, H. (2021). In vivo delivery of CRISPR–Cas9 therapeutics: Progress and challenges. *Acta Pharm. Sin. B* 11, 2150–2171. <https://doi.org/10.1016/j.apsb.2021.05.020>.
 44. Li, K., Wang, C., Yang, F., Cao, W., Zhu, Z., and Zheng, H. (2021). Virus–Host Interactions in Foot-and-Mouth Disease Virus Infection. *Front. Immunol.* 12, 571509. <https://doi.org/10.3389/fimmu.2021.571509>.
 45. Letunic, I., and Bork, P. (2019). Interactive Tree Of Life (iTOL) v4: recent updates and new developments. *Nucleic Acids Res.* 47, W256–W259. <https://doi.org/10.1093/nar/gkz239>.
 46. Katoh, K., and Standley, D.M. (2013). MAFFT Multiple Sequence Alignment Software Version 7: Improvements in Performance and Usability. *Mol. Biol. Evol.* 30, 772–780. <https://doi.org/10.1093/molbev/mst010>.
 47. Jagla, B., Aulner, N., Kelly, P.D., Song, D., Volchuk, A., Zatorski, A., Shum, D., Mayer, T., de Angelis, D.A., Ouerfelli, O., et al. (2005). Sequence characteristics of functional siRNAs. *RNA* 11, 864–872. <https://doi.org/10.1261/rna.7275905>.
 48. Reynolds, A., Leake, D., Boese, Q., Scaringe, S., Marshall, W.S., and Khvorovova, A. (2004). Rational siRNA design for RNA interference. *Nat. Biotechnol.* 22, 326–330. <https://doi.org/10.1038/nbt936>.

49. Peek, A.S. (2007). Improving model predictions for RNA interference activities that use support vector machine regression by combining and filtering features. *BMC Bioinf.* 8, 182. <https://doi.org/10.1186/1471-2105-8-182>.
50. Vert, J.-P., Foveau, N., Lajaunie, C., and Vandembrouck, Y. (2006). An accurate and interpretable model for siRNA efficacy prediction. *BMC Bioinf.* 7, 520. <https://doi.org/10.1186/1471-2105-7-520>.
51. Liu, Q., Zhou, H., Cui, J., Cao, Z., and Xu, Y. (2012). Reconsideration of In-Silico siRNA Design Based on Feature Selection: A Cross-Platform Data Integration Perspective. *PLoS One* 7, e37879. <https://doi.org/10.1371/journal.pone.0037879>.
52. Klingelhofer, J.W., Moutsianas, L., and Holmes, C. (2009). Approximate Bayesian feature selection on a large meta-dataset offers novel insights on factors that effect siRNA potency. *Bioinformatics* 25, 1594–1601. <https://doi.org/10.1093/bioinformatics/btp284>.
53. Shabalina, S.A., Spiridonov, A.N., and Ogurtsov, A.Y. (2006). Computational models with thermodynamic and composition features improve siRNA design. *BMC Bioinf.* 7, 65. <https://doi.org/10.1186/1471-2105-7-65>.
54. Khvorova, A., Reynolds, A., and Jayasena, S.D. (2003). Functional siRNAs and miRNAs Exhibit Strand Bias. *Cell* 115, 209–216. [https://doi.org/10.1016/S0092-8674\(03\)00801-8](https://doi.org/10.1016/S0092-8674(03)00801-8).
55. Naito, Y., Yoshimura, J., Morishita, S., and Ui-Tei, K. (2009). siDirect 2.0: updated software for designing functional siRNA with reduced seed-dependent off-target effect. *BMC Bioinf.* 10, 392. <https://doi.org/10.1186/1471-2105-10-392>.
56. Viol, D.I., Chagonda, L.S., Moyo, S.R., and Mericli, A.H. (2016). Toxicity and Antiviral Activities of Some Medicinal Plants Used by Traditional Medical Practitioners in Zimbabwe. *Am. J. Plant Sci.* 07, 1538–1544. <https://doi.org/10.4236/ajps.2016.711145>.